SPREADING OF A TURBULENT JET IMPINGING ON A FLAT SURFACE

O. V. Yakovlevskii and S. Yu. Krasheninnikov

Izv. AN SSSR. Mekhanika Zhidkosti i Gaza, Vol. 1, No. 4, pp. 192–197, 1966

1. The tests were conducted using a setup which permitted studying the spreading of an air jet over a disc of 400-mm diameter. The jet impacted on the disc at angles of 30, 45, 60, and 90°, and the distance l from the nozzle exit to the disc along the jet axis was 35 and 100 mm for a nozzle radius $R_0 = 5$ mm. Thus, the flow studied corresponded to impact of a jet with a deflector both in its initial segment ($l^\circ = l/R_0 = 7$) and in the primary segment ($l^\circ = 20$). A system of traversing probes permitted determination of the velocity head field along any direction on the plane of the disc and traversal of this field along the vertical (the disc was placed horizontally). The total head probe positioning accuracy was 0.5 mm. The air flowrate was established with the aid of a calibrated orifice with an accuracy of 2–3%. The air velocity at the nozzle exit was not varied during the tests and was 103 m/sec. The velocity head fields were determined from the indications of an alcohol micromanometer with an accuracy of 0.2 mm H_2O. Pressure taps were located every 5 mm along the radius of the disc for measuring the static pressure. The velocity head fields were measured on radii making angles $\psi = 0$, 45, 90, 135, and 180° with the projection of the jet axis on the disc. These radii were drawn from the point of intersection O_ψ on the jet axis with the plane of the disc.

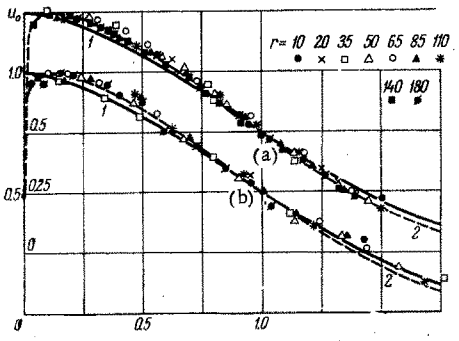

Fig. 1. Distribution of relative velocity u° along jet thickness. a) $\theta = 90°$, $l^\circ = 7$; b) $\theta = 45°$, $l^\circ = 7$, $\psi = 0°$. 1) Schlichting profile; 2) same with account for boundary layer.

The results of the measurement of the velocity distribution along the vertical at various points of the disc are shown in Fig. 1. We can see that the relative velocity profiles in the coordinates u°, z° are similar. As the characteristic scales for the velocity and length in the expressions $u^\circ \equiv u/u_m$ and $z^\circ \equiv z/z_{0.5}$ we have used the maximal velocity u_m at the given point of the disc and the half-thickness $z_{0.5}$ of the jet, corresponding to the distance along the vertical from the disc surface to the point at which $u = 0.5\, u_m$.

Figure 1 shows that the velocity profile is described well by the Schlichting formula

$$u^\circ = (1 - \xi^{3/2})^2 \quad \text{for} \quad z \geqslant \delta, \qquad \xi = \frac{z - \delta}{b - \delta}.$$
$$u^\circ = (z/\delta)^{1/n} \quad \text{for} \quad z \leqslant \delta$$

Here δ is the boundary layer thickness, b is the jet thickness (n was not determined in the experiments, but from the data of [4] for semi-bounded jets $n \approx 10$).

Figure 2 shows the dependence of the quantity $z_{0.5}$ on the radius r, the distance from the point O_ψ, for various impact angles θ. On the basis of the Schlichting velocity profile (with account for the boundary layer) we can obtain the dependence $-16(-)-16$ of the jet thickness on r

$$\frac{b - b_*(\psi)}{r - r_*(\psi)} = c \approx 0.16, \tag{1.1}$$

where $b_*(\psi)$ and $r_*(\psi)$ are the initial values of the jet thickness and the radius. Here we have made use of the fact that the relation $z_{0.5} = (0.44–0.5)b$ obtains for the velocity profile presented above as a function of the boundary layer thickness. Measurements showed that the boundary layer thickness (distance from the disc surface to the point where the velocity is maximal) was 5–10% of the jet thickness in the tests conducted.

The distribution of the maximal velocities in the plane of the disc (Fig. 3) was constructed from the measurement results. We see that the shape of the isotachs does not differ greatly from circular with approach to the point O_ψ. Figure 4 shows the data characterizing the decrease of the maximal velocity u_m° with increasing distance from the impact region.

2. The experimental data obtained formed the basis for a flow pattern which made it possible to carry out its approximate calculation. Figure 5 shows a schematic picture of jet spreading which was used as a basis for the calculation. We shall list the salient features of the flow model used for the calculation. The basic assumption, which is to some degree confirmed by the data of Fig. 3, is that after rotation of the jet the flow is realized in the form which would have taken place with discharge from a cylindrical circular source of variable height b_*. The center O_φ of this source is shifted by the amount Δ (see Fig. 5) relative to the point O_ψ of intersection of the jet axis and the plane of the deflector. The velocity at the exit from the source is constant and equal to u_{m*}. The discharge takes place in the direction of the radii drawn from O (this is confirmed by the measurement data).

The static pressure measurements showed that near the deflection zone (outside the source) it differs from the atmospheric pressure by no more than 2–3% of the maximal velocity head at the corresponding point of the disc; with further removal from O_ψ it approaches atmospheric pressure. This circumstance makes it possible to assume that the jet remains isobaric as it spreads over the deflector.

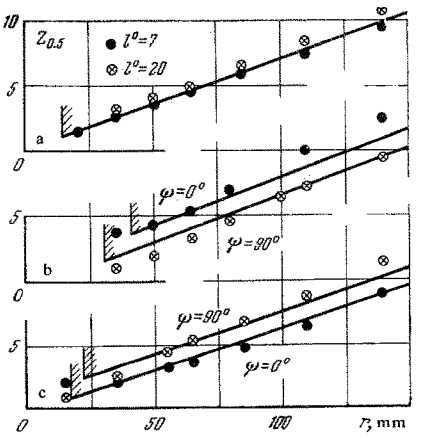

Fig. 2. Variation of jet half-thickness $z_{0.5}$ with increased distance from the turning zone: a) $\theta = 90°$; b) $\theta = 60°$, $l^\circ = 20$; c) $\theta = 45°$, $l^\circ = 7$. Vertical line with shading corresponds to $r = r_*$.

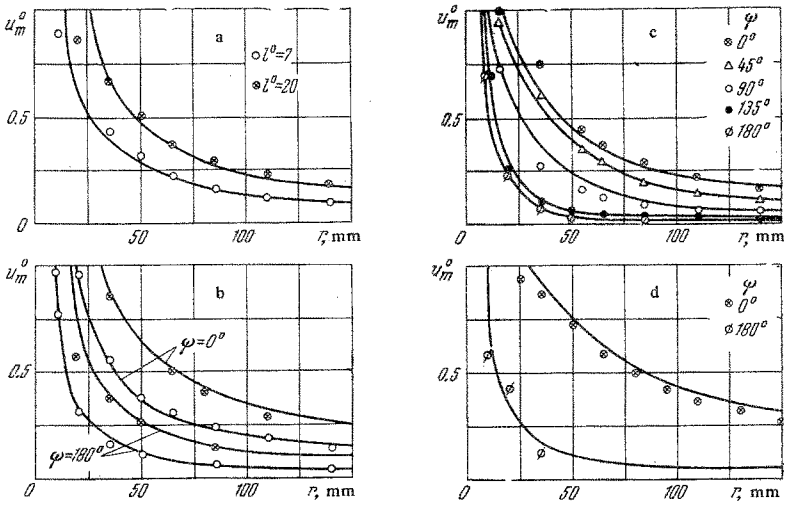

Fig. 4. Decay of maximal velocity u_m^0 with distance from the turning zone.
a) θ = 90°; b) θ = 60°, l^0 = 20, l^0 = 7; c) θ = 45°, l^0 = 7; d) θ = 30°, l^0 = 20.

In line with the experimental data, we can assume that the upper base of the cylindrical source is a plane which forms an angle with the plane of the deflector. In this case the height of the generating lines of the annular source as a function of the direction of spreading is expressed by the relation

$$b_* = A + B\cos\varphi. \tag{2.1}$$

The angle φ differs from the angle ψ by the amount ε, which depends on ψ (Fig. 5).

To determine the flow at the outlet of the source it is necessary to find the three geometric parameters A, B, and Δ, which depend on the angle θ of incidence of the jet on the plane of the deflector, the shape of the longitudinal velocity profile in the free jet ahead of the turning zone, and the single kinematic parameter u_{m*}, which depends on the magnitude and distribution of the velocity w at the entrance to the annular source. The jet parameters directly ahead of the turning zone, which may be identified approximately with the annular source, are determined by the known laws for a turbulent jet [5]. This is justified by the fact that the presence of the deflector does not have a significant influence on the flow in the jet up to the turning zone itself [1].

3. To determine the magnitude of the maximal velocity at the exit from the annular source we assume that the total flowrate and the stream kinetic energy are conserved in the turning process, i.e.,

$$\int_{t_*}^{b_*}\int_0 u\cos\varepsilon\,dz\,dt = \int_{s_*} w r\,ds,$$
$$\int_{t_*}^{b_*}\int_0 u^3\cos\varepsilon\,dz\,dt = \int_{s_0} w^3 r\,ds. \tag{3.1}$$

Here ε is the angle between the radii-vectors $\vec{r}$ and $\vec{\rho}$, drawn in the plane of the deflector respectively from the points O_ψ and O_φ (see Fig. 5); t_* is the boundary of the base of the annular source; b_* is the height of the cylinder generators; z is the coordinate axis normal to the deflector plane; s_0 is the cross-sectional area of the jet at the entrance to the turning zone. Assuming that the velocity profiles are independent of φ, i.e.,

$$u_*(z^\circ) = u_{m*} f(z^\circ),\ z^\circ = z/b_*,\ w_*(R^\circ) = w_{m*} f_0(R^\circ),\ R^\circ = R/R_*, \tag{3.2}$$

we transform relation (3.1) to the form

$$\int_0^1 f(z^\circ)\,dz^\circ \int_{t_*} b_* u_{m_*}\cos\varepsilon\,dt = \pi R_*^2 \int_0^1 f_0(R^\circ) R^\circ w_{m*}\,dR^\circ,$$
$$\int_0^1 f^3(z^\circ)\,dz^\circ \int_{t_*} b_* u_{m*}^3\cos\varepsilon\,dt = \pi R_*^2 \int_0^1 f_0^3(R^\circ) R^\circ w_{m*}^3\,dR^\circ. \tag{3.3}$$

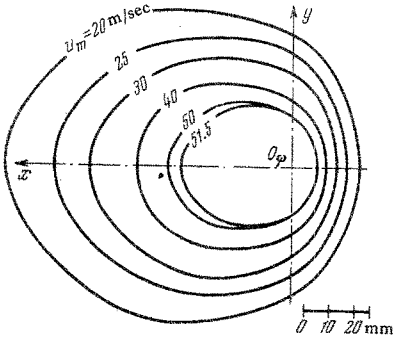

Fig. 3. Lines of constant maximal velocities for θ = 45° and l^0 = 20.

Here R is the radial distance from the axis of the free jet to an arbitrary point; R_* is the boundary radius of the free jet ahead of the turning zone; w_{m*} is the maximal velocity (on the axis) in the jet ahead of the turning zone; and u_{m*} is the maximal velocity at the exit from the annular source (independent of φ). Solving (3.3), we obtain

$$u_{m*} = \alpha w_{m*}, \tag{3.4}$$

$$\alpha = \left(\int_0^1 f_0^3(R^\circ) R^\circ\,dR^\circ \int_0^1 f(z^\circ)\,dz^\circ\right)^{1/2} \times$$
$$\times \left(\int_0^1 f_0(R^\circ) R^\circ\,dR^\circ \int_0^1 f^3(z^\circ)\,dz^\circ\right)^{-1/2}. \tag{3.5}$$

(In the case of the Schlichting profile α = 0.778)

To find the parameters A and B in (2.1) we make use of the conditions of conservation of mass flowrate and the projection of the momentum on the deflector plane. Using (2.1), (3.2), and (3.5), these conditions may be written in the form

$$2\rho\int_0^\pi (A + B\cos\varphi)\cos\varepsilon\,d\varphi = \frac{s_0}{\alpha}\beta,$$
$$2\rho\int_0^\pi (A + B\cos\varphi)\cos\varepsilon\cos\psi\,d\varphi = \frac{s_0}{\alpha^2}\gamma\lambda. \tag{3.6}$$

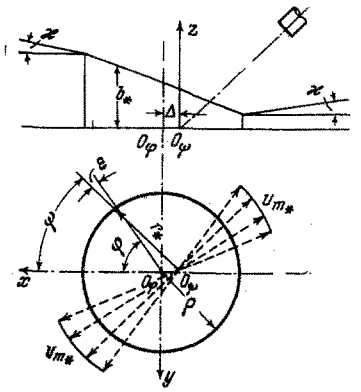

Fig. 5. Jet spreading pattern.

Here the following notations are introduced in addition to the radius ρ of the annular source: $\lambda = \cos\theta$,

$$\beta = 2\left(\int_0^1 f_0(R^\circ)\,R^\circ\,dR^\circ\right)\left(\int_0^1 f(z^\circ)\,dz^\circ\right)^{-1},$$

$$\gamma = 2\left(\int_0^1 f_0^2(R^\circ)\,R^\circ\,dR^\circ\right)\left(\int_0^1 f^2(z^\circ)\,dz^\circ\right)^{-1}.$$

Taking account of the geometric rotation pattern, we can write the relation

$$\cos\varepsilon = \frac{\mathbf{r}\,\boldsymbol{\rho}}{|\mathbf{r}|\cdot|\boldsymbol{\rho}|}, \quad \text{or} \quad \cos\varepsilon = \frac{\rho + \Delta\cos\varphi}{\sqrt{\rho^2 + 2\rho\Delta\cos\varphi + \Delta^2}}. \tag{3.7}$$

Using the resulting relations and neglecting the variation of $\cos\varepsilon$ in comparison with the variation of $\cos\psi$, we can obtain the mass flowrate and momentum equations in the form

$$A(I_0 + \Delta^\circ I_1) + B(I_1 + \Delta^\circ I_2) = \frac{s_0}{2\rho\alpha}\beta,$$

$$A(I_1 + \Delta^\circ I_0) + B(I_2 + \Delta^\circ I_1) = \frac{s_0\gamma\lambda}{2\rho\alpha^2}. \tag{3.8}$$

Here the following notations are used:

$$\Delta^\circ = \frac{\Delta}{\rho}; \qquad I_i = \int_0^\pi \frac{\cos^i\varphi\,d\varphi}{\sqrt{1 + 2\Delta^\circ\cos\varphi + \Delta^{\circ 2}}} \qquad (i = 0, 1, 2.).$$

Calculations show that

$$A = \frac{s_0\beta}{2\rho\alpha(I_0 + \Delta^\circ I_1)} \quad (0 \leqslant \Delta^\circ \leqslant 0.85), \quad A = \frac{s_0\beta}{2\rho\alpha\pi} \quad (\Delta^\circ < 0.6). \tag{3.9}$$

This result indicates that the average height of the turning zone is practically independent of the angle at which the jet impinges on the deflector.

In order to find the fourth unknown quantity Δ°, the system of conservation equations must be closed by still another relation. In calculating the turning of an ideal fluid jet [6], the assumption is made that mass flowrate is conserved in an angular element before and after the turning zone. A similar assumption, only in integral form, may be made in the present case. Figure 6 shows the cross section of the jet ahead of the turning zone and the base of the cylinder of the annular source. Drawing in the plane of the cylinder base through O_ψ the line $a - a$ perpendicular to the x axis, we divide the fluid stream into two parts: all the fluid located to the right of $a - a$ will move to the right, and all the fluid to the left of this line will move to the left. In the cross section s_0 of the jet at some distance Δ' from the jet axis we can also draw the line $a' - a'$ perpendicular to the x axis, concerning which, we can say the same as for the line $a - a$; the fluid to the left of $a' - a'$ moves to the left after turning, while the fluid to the right of $a' - a'$ moves to the right. Let us assume, by analogy with the ideal fluid theory, that the distances Δ and Δ' are proportional to the radii of the corresponding circles

$$\frac{\Delta'}{R_*} = \frac{\Delta}{\rho} \equiv \Delta^\circ. \tag{3.10}$$

This relation closes the system.

On the basis of the flow pattern assumed, we can write the mass balance equation. With account for the second of relations (3.9) and (3.10), and also neglecting the variation of $\cos\varepsilon$, the condition of equality of the mass flows through the unshaded portion of the sections (Fig. 6) yields

$$B\sqrt{1 - \Delta^{\circ 2}} = \frac{R_*^2 w_{m*}}{\rho u_{m*}}\left(\int_0^1 f(z^\circ)\,dz^\circ\right)^{-1} \times$$

$$\times \int_0^{\arccos\Delta^\circ} \int_0^{\Delta^\circ/\cos\omega} f_0(R^\circ)\,R^\circ\,dR^\circ d\omega. \tag{3.11}$$

The angle ω is measured from the negative direction of the x axis, i.e., $\omega = \pi - \varphi$.

Joint solution of (3.8) and (3.11) permits finding the quantities B and Δ° as a function of λ and the shape of the velocity profiles in the jet ahead of the turning zone.

Calculations have shown that for a wide range of values of λ the following relation is well satisfied:

$$\Delta^\circ = \frac{\Delta}{\rho} = \lambda\left(2\int_0^1 f_0(R^\circ)\,R^\circ dR^\circ\right)^{1/4}. \tag{3.12}$$

For the ideal fluid jet (rectangular velocity profile) Eq. (3.12) becomes the relation $\Delta^\circ = \lambda$ obtained by Schach [6].

Using the results obtained above, we write out the final equations for calculating the parameters of the annular source:

$$u_{m_*} = \alpha w_{m_*}, \quad A^\circ = \frac{\beta\pi}{2\alpha(I_0 + \Delta^\circ I_1)} \quad \left(A^\circ \approx \frac{\beta}{2\alpha} \quad \text{for} \quad \Delta^\circ < 0.6\right),$$

$$B^\circ = \frac{-A^\circ[\Delta^\circ I_0 + I_1] + {}^1/_2\pi\gamma\lambda\alpha^{-2}}{I_2 + \Delta^\circ I_1}, \quad \Delta^\circ = \lambda\left(2\int_0^1 f_0(R^\circ)\,R^\circ\,dR^\circ\right)^{1/4},$$

$$A^\circ = kA/R_*, \qquad B^\circ = kB/R_*, \qquad k = \rho/R_*. \tag{3.13}$$

The approximating equation (3.12) for Δ° may be used in the range of values $0 \leq \lambda \leq 0.7$ which corresponds to impact angles $90^\circ \geq \theta \geq 45^\circ$. For large values of λ the quantity Δ° may be obtained either by numerical integration or by extrapolation with the use of the condition $\lambda = 1$, $\Delta^\circ = 1$.

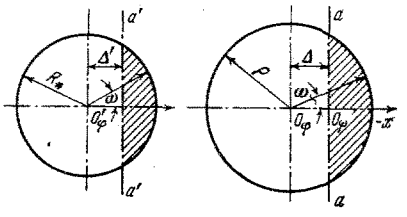

Fig. 6. Diagram for determining mass flowrate balance.

The quantity k introduced above is an experimental constant. It was determined from the condition of best correspondence of the quantities b_* and r_* in relation (1.1) when drawing the lines corresponding to $z_{0.5}$ in Fig. 2 and was found to be equal to 1.5. The quantities b_* and r_* are connected by relations (3.13) since condition (2.1) holds.

4. To calculate the further spreading of the jet over the plane we can use the experimental relations (1.1). Let us consider the motion of a fluid element in cylindrical coordinates in which the z axis is

directed perpendicular to the deflector plane, and the coordinate origin is at the point O_ψ. We write the momentum variation law for an elementary fluid volume of length dr bounded by two planes, with the angle $d\psi$ between them, which pass through the z axis

$$\int_0^{b_1} u_1^2 dz_1 dL_1 = \int_0^{b_2} u_2^2 dz_2 dL_2 + T dF_1 - (Q - Q')\, dF_2. \qquad (4.1)$$

Here b is the element height; L is the arc bounding the element; T is the friction stress on the lower face of the element F_1; Q and Q' are the turbulent shear stresses on the lateral faces F_2. (The effect of the pressure forces cancels out.) Letting the longitudinal and lateral dimensions of the isolated element approach zero, and also using Eq. (1.1), the geometric relations

$$b_1 = (r - r_*)c + b_*, \quad b_2 = (r + dr - r_*)\, c + b_*,$$

$$dL_1 = r d\psi, \quad dL_2 = (r + dr)\, d\psi,$$

and the similarity condition for the velocity profiles, after discarding terms of second order of smallness, we obtain the following differential equation:

$$r\,[(r - r_*)c + b_*]\frac{du_m^2}{dr} - u_m^2\,[(2r - r_*)c + b_*] - \frac{T}{J} + \frac{b}{J}\frac{dQ}{d\psi} = 0$$

$$\left(J = \int_0^1 f^2(z^\circ)\, dz^\circ\right). \qquad (4.2)$$

Estimates have shown that the third term of (4.2) for the value $R = 7 \cdot 10^4$ of the Reynolds number (calculated from the nozzle diameter and the flow parameters) which obtained in the experiments is no more than 4.5% of the magnitude of the left side. For large values of the Reynolds number, which are to be expected in cases of practical interest, this term is still smaller. The maximal value of the fourth term does not exceed 2.5% of the sum of the terms of the left side. After neglecting these terms, Eq. (4.2) may be integrated with the use of the condition

$$r = r_*, \qquad u_m = u_{m^*} = \alpha w_{m^*}.$$

Thus, we obtain

$$u_m^2 = \alpha^2 w_{m*}^2 \cdot \frac{r_*}{r}\left[1 + \frac{ck^2}{A^\circ + B^\circ \cos\varphi}\left(\frac{r}{r_*} - 1\right)\right]^{-1},$$

$$r_* = \rho\,(\sqrt{1 + \Delta^{\circ 2}\sin^2\psi} + \Delta^\circ \cos\psi),$$

$$\cos\varphi = -\Delta^\circ \sin^2\psi + \cos\psi\,\sqrt{1 + \Delta^{\circ 2}\sin^2\psi}. \qquad (4.3)$$

The parameters A°, B°, Δ° and α are found from (3.13), (3.12), and (3.5). The angle determining the direction of the spreading is ψ; the angle φ plays an auxiliary role and serves to describe the geometric pattern of the turning.

If in the free jet prior to impact on the deflector the maximal velocity on the jet axis $w_m \sim 1/l$ and the jet radius $R \sim l$, which corresponds to the experimental conditions, it follows from (4.3) that for sufficiently large r the value of the maximal velocity u_m at any point of the deflector is independent of l and is determined only by the angle θ. This fact is confirmed by the experiments conducted in our study.

The case of direct jet impact on the plane ($\theta = 90°$), which is considered in [1], is obtained for $B^\circ = 0$. In this case the first of Eqs. (4.3) becomes the corresponding relation obtained in [1].

5. In order to make use of the equations for calculating the flow over the deflector, it is necessary to know the parameters of the jet ahead of the turning zone. These parameters are determined using known equations presented, for example, in [1]

$$w_{m^*}/w_{m_0} = 1, \quad R_*/R_0 = k_2' l^\circ + 1 \text{ for } l^\circ \leqslant 12,$$

$$w_{m^*}/w_{m_0} = k_2/l^\circ, \quad R_*/R_0 = k_2 l^\circ \text{ for } l^\circ \geqslant 12,$$

$$k_2 = 0.22, \quad k_2' = 0.14, \quad k_3 = 12.4.$$

When determining the velocity profile at the entrance to the turning zone in the case $l < 12$ we need to know the ordinate of the inner boundary of the mixing zone R_1, which is determined from the equation $(R_0 - R_1)/R_0 = 0.13\, l^\circ$.

To calculate the quantities α, β, and γ in the initial portion of the jet we can use the relation

$$\int_0^1 f_0^n(R^\circ)\, R^\circ dR^\circ = 0{,}5\,(R_1^\circ)^2 + (1 - R_1^\circ)^2 \int_0^1 f_{00}^n(\eta)\,\eta d\eta +$$

$$+ (1 - R_1^\circ)\, R_1^\circ \int_0^1 f_{00}^n(\eta)\, d\eta, \qquad R_1^\circ = \frac{R_1}{R_*}, \qquad \eta = \frac{R - R_1}{R_* - R_1}.$$

In the calculations made in the present study we used the Schlichting formula to describe the velocity profile ahead of the turning zone

$$f_{00}(\eta) = (1 - \eta^{3/2})^2.$$

To describe the velocity profile at the exit from the annular source and in the further spreading of the jet over the deflector we used the Schlichting profile with account for the boundary layer (see Fig. 1)

$$u^\circ = (z/\delta)^{1/n} \quad \text{for} \quad z \leqslant \delta;$$

$$u^\circ = [1 - (z - \delta)^{3/2}(b - \delta)^{-3/2}]^2 \quad \text{for} \quad \delta \leqslant z \leqslant b.$$

The location of the upper base of the annular source is not known ahead of time, therefore the calculation of the parameters of the free jet ahead of the impact zone is made using successive approximations. First the geometric parameters of the turning zone, the annular source, are calculated as a function of the distance l from the nozzle to the deflector; then a correction is introduced for the finite thickness of the turning zone. Usually two approximations are quite adequate.

The results of the calculations are shown together with the experimental data on the decay of the maximal velocity $u_m^\circ u_m / w_{m^*}$ in Fig. 4. Comparison indicates satisfactory agreement.

In conclusion the author wishes to thank G. B. Krayushkin who aided in the experiments and presentation of the results of the study.

REFERENCES

1. O. V. Yakovlevskii and A. N. Sekundov, "Study of the interaction of a jet with nearby deflectors," Izv. AN SSSR, Mekhan. i mashin., no. 1, 1964.

2. G. G. Shamtsiyan, "On admissible temperature of a jet of cold air entering a room," Vodosn. i san. tekhnika, no. 9, 1963.

3. A. T. Sychev, "Results of a study of a submerged turbulent jet incident on the surface of a smooth ceiling," Inzh.-fiz. zh., 7, no. 3, 1964.

4. Z. B. Sakipov, "Experimental study of semibounded jets," collection: Problems of Thermoenergetics and Applied Thermophysics [in Russian], no. 1, Applied Thermophysics, Izd. AN KazSSR, Alma Ata, 1964.

5. G. N. Abramovich, Theory of Turbulent Jets [in Russian], Moscow, Fizmatgiz, 1960.

6. W. Schach, Umlenkung eines freien Flussigkeitsstrahles an einer ebenen Platte, Ing.-Archiv, **5**, no. 4, 1934.

30 November 1965 Moscow